CrossMark

$N − 1$ modal interactions of a three-degree-of-freedom system with cubic elastic nonlinearities

X. Liu · A. Cammarano · D. J. Wagg · S. A. Neild · R. J. Barthorpe

Abstract In this paper the $N − 1$ nonlinear modal interactions that occur in a nonlinear three-degree-of-freedom lumped mass system, where $N = 3$, are considered. The nonlinearity comes from springs with weakly nonlinear cubic terms. Here, the case where all the natural frequencies of the underlying linear system are close (i.e. $\omega_{n1} : \omega_{n2} : \omega_{n3} \approx 1 : 1 : 1$) is considered. However, due to the symmetries of the system under consideration, only $N − 1$ modes interact. Depending on the sign and magnitude of the nonlinear stiffness parameters, the subsequent responses can be classified using backbone curves that represent the resonances of the underlying undamped, unforced system. These backbone curves, which we estimate analytically, are then related to the forced response of the system around resonance in the frequency domain. The forced responses are computed using the continuation software AUTO-07p. A comparison of the results gives

insights into the multi-modal interactions and shows how the frequency response of the system is related to those branches of the backbone curves that represent such interactions.

1 Introduction

Understanding the effects of modal interactions of coupled systems of nonlinear equations is an important step in being able to predict the subsequent dynamic response of the system. In this paper, we consider a three-degree-of-freedom (3-DoF) lumped mass system with cubic stiffness nonlinearities. In particular we consider the potential forced responses that can occur by analysing the backbone curves of the underlying undamped, unforced system. The justification of this approach lies in that the vast majority of engineering structures is characterised by low level of damping. This implies that their dynamical behaviour is largely determined by the dynamics of the associated Hamiltonian system [10].

The motivation for this study is the possibility for modes, in multi-degree-of-freedom nonlinear systems, to interact with each other [17]. These types of modal interaction have been previously studied because they are often related to unwanted vibration effects in engineering structures [16]. The majority of

X. Liu (✉) · D. J. Wagg · R. J. Barthorpe
Department of Mechanical Engineering, University of Sheffield, Sheffield S1 3JD, UK
e-mail: xuanang.liu@sheffield.ac.uk

D. J. Wagg
e-mail: david.wagg@sheffield.ac.uk

A. Cammarano
School of Engineering, University of Glasgow, Glasgow G12 8QQ, UK

S. A. Neild
Department of Mechanical Engineering, University of Bristol, Bristol BS8 1TR, UK

Fig. 1 A schematic diagram of the in-line 3-DoF oscillator system
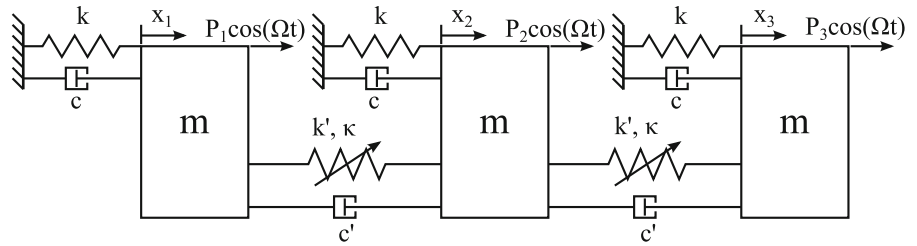
the existing literature is for undamped, unforced systems, and includes structural elements such as beams, cables, membranes, plates and shells—see for example [1,15,27]. Several different analytical and numerical approaches have been used to approach this type of problem, such as perturbation methods [18], nonlinear normal modes [13,22,23,25] or normal form analysis [2,11,21]. The majority of work in the literature on modal interaction is based on 2-DoF nonlinear systems where two modes interact, see for example [3,5,8–10,13,29], although for continuous systems higher numbers of modes can typically be retained in the approximation, see for example [24]. Some work has been carried out on 3-DoF lumped mass systems in the context of nonlinear vibration suppression [12].

In a system with N modes, it is possible for response solutions to exist in which some (i.e. $N - i \geq 2$) and/or all N of the modes interact. In this paper, we consider the case where this type of $N - i$ modal interaction can occur. More specifically, the case where $N = 3$ is analysed, i.e. only two (i.e. $N - 1$) modes can interact. To do this we have chosen a specific configuration of an in-line 3-DoF nonlinear oscillator with small forcing and light damping. Due to the structural symmetry, one of the modes of this system is linear and the other two modes are nonlinear. So even though all the modal natural frequencies are close, the linear mode is not coupled with the other two. Hence the study of the 3-DoF system is reduced to the modal interaction of two coupled modes. Our analysis follows the approach developed by [3,9] to consider nonlinear modal interactions of a 2-DoF nonlinear oscillator. However, the effects of two modes interacting in this 3-DoF system has subtle differences from those described in the previous literature. This will be explained in Sect. 4.

The paper is structured as follows. In Sect. 2 we describe the configuration of this in-line oscillator. Then, we apply a normal form transformation method to the 3-DoF system to obtain its potential backbone curves expressions. In Sect. 3 the backbone curves of

the system with the hardening nonlinearity are computed. These curves are then used to infer the dynamic behaviour of the system, which in turn can be used to interpret the forced, damped behaviour. In the Sect. 4, the backbone curves of the system with softening nonlinearity are presented. Lastly, the stability of the backbone branches are analysed and their relation with the forced response are shown. Conclusions are drawn in Sect. 5.

2 System description and analytical method application

The example system considered here is shown in Fig. 1. It consists of three lumped masses which are all grounded via linear springs, k, and viscous dampers, c. The mass in the middle links the two masses at two sides via the linear viscous dampers, c', and the cubic nonlinear springs. The elastic force characteristics of these nonlinear springs is $F = k'(\Delta x) + \kappa(\Delta x)^3$. Each of the masses is harmonically forced at the same frequency, Ω, and at the amplitude, P_i. The equations of motion for this system are written in the form,

$$\mathbf{M}\ddot{\mathbf{x}} + \mathbf{K}\mathbf{x} + \mathbf{N}_x(\mathbf{x}, \dot{\mathbf{x}}) = \mathbf{P}_x \cos(\Omega t), \qquad (1)$$

where $\mathbf{x}, \dot{\mathbf{x}}$ and $\ddot{\mathbf{x}}$ are the physical displacement, velocity and acceleration vectors, respectively. $\mathbf{K}$ is the linear stiffness matrix, $\mathbf{P}_x$ is the external force amplitude vector and $\mathbf{N}_x(\mathbf{x}, \dot{\mathbf{x}})$ contains the nonlinear and damping terms which are assumed to be small. Their expressions are,

$$\mathbf{K} = \begin{bmatrix} k + k' & -k' & 0 \\ -k' & k + 2k' & -k' \\ 0 & -k' & k + k' \end{bmatrix}, \qquad \mathbf{P}_x = \begin{pmatrix} P_1 \\ P_2 \\ P_3 \end{pmatrix},$$

and

$$\mathbf{N}_x = \begin{bmatrix} c + c' & -c' & 0 \\ -c' & c + 2c' & -c' \\ 0 & -c' & c + c' \end{bmatrix} \dot{\mathbf{x}} + \kappa$$

$$\begin{pmatrix} (x_1 - x_2)^3 \\ (x_2 - x_1)^3 + (x_2 - x_3)^3 \\ (x_3 - x_2)^3 \end{pmatrix}.$$

To proceed, the second-order normal form method is applied to approximately solve the equations of motion of this system. First, in order to decouple the linear terms, the linear modal transformation is applied to Eq. 1 to obtain the linear modal decomposition equations in terms of the new modal state $\mathbf{q} = \{q_1 \ q_2 \ q_3\}^T$ as,

$$\ddot{\mathbf{q}} + \Lambda \mathbf{q} + \mathbf{N}_q(\mathbf{q}, \dot{\mathbf{q}}) = \mathbf{P}_q \cos(\Omega t), \qquad (2)$$

where Λ is a diagonal matrix of the squares of the corresponding linear natural frequencies $\omega_{n1}^2 = k/m$, $\omega_{n2}^2 = (k + k')/m$ and $\omega_{n3}^2 = (k + 3k')/m$. $\mathbf{N}_q$ is the vector containing the damping and nonlinear coupling terms,

$$\mathbf{N}_q = \begin{pmatrix} 2\omega_{n1}\zeta_1\dot{q}_1 \\ 2\omega_{n2}\zeta_2\dot{q}_2 \\ 2\omega_{n3}\zeta_3\dot{q}_3 \end{pmatrix} + \mu \begin{pmatrix} 0 \\ q_2^3 + 27q_2q_3^2 \\ 9q_2^2q_3 + 27q_3^3 \end{pmatrix}, \qquad (3)$$

where $\mu = \kappa/m$, $2\omega_{n1}\zeta_1 = c/m$, $2\omega_{n2}\zeta_2 = (c+c')/m$ and $2\omega_{n3}\zeta_3 = (c + 3c')/m$. In the modal coordinates, the external force amplitude vector, $\mathbf{P}_q = \{P_{m1} \ P_{m2} \ P_{m3}\}^T$, is

$$\mathbf{P}_q = \Phi^{-1}\mathbf{M}^{-1}\mathbf{P}_x = \frac{1}{6m} \begin{bmatrix} 2 & 2 & 2 \\ 3 & 0 & -3 \\ 1 & -2 & 1 \end{bmatrix} \mathbf{P}_x, \qquad (4)$$

where Φ is the matrix of the linear modeshapes. Here the modeshapes used for the linear transformation are $\{1, \ 1, \ 1\}^T, \{1, \ 0, \ -1\}^T$ and $\{1, \ -2, \ 1\}^T$ for the three modes, respectively.

Then, the forcing transformation, $\mathbf{q} \to \mathbf{v}$, is supposed to be applied to remove the non-resonant forcing terms. Here we assume that the system is forced near resonance, this allows us to set $\mathbf{q} = \mathbf{v}$. Substituting this into Eq. 2 gives,

$$\ddot{\mathbf{v}} + \Lambda\mathbf{v} + \mathbf{N}_v(\mathbf{v}, \dot{\mathbf{v}}) = \mathbf{P}_v \cos(\Omega t), \qquad (5)$$

where $\mathbf{N}_v(\mathbf{v}, \dot{\mathbf{v}}) = \mathbf{N}_q(\mathbf{q}, \dot{\mathbf{q}})$ and $\mathbf{P}_v = \mathbf{P}_q$.

Lastly, applying the near-identity nonlinear transform $\mathbf{v} \to \mathbf{u}$ to Eq. 5 by using $\mathbf{v} = \mathbf{u} + \mathbf{H}(\mathbf{u}, \dot{\mathbf{u}})$ gives the equation,

$$\ddot{\mathbf{u}} + \Lambda\mathbf{u} + \mathbf{N}_u(\mathbf{u}, \dot{\mathbf{u}}) = \mathbf{P}_u \cos(\Omega t), \qquad (6)$$

where $\mathbf{P}_u = \mathbf{P}_q$ and $\mathbf{N}_u = \mathbf{n}_u\mathbf{u}^*$ includes only the nonlinear resonant terms responding at the fundamental frequency of the corresponding modes. Here $\mathbf{u}$ and

$\mathbf{H}(\mathbf{u}, \dot{\mathbf{u}})$ used in the transformation are the fundamental and harmonic components of $\mathbf{v}$, respectively. Substituting $v_i \to u_i = u_{ip} + u_{im}$ into Eq. 3 in $\mathbf{v}$ gives the functional form of the $\mathbf{u}^*$ vector and the coefficient matrix $\mathbf{n}_v$ so that $\mathbf{N}_v = \mathbf{n}_v\mathbf{u}^*$ as below, where the subscript i represents the ith linear mode.

Then the homological equation is used to compute a matrix, $\boldsymbol{\beta}$, for determining the resonance terms in the near-identity transformation [21]. The individual $\beta_{i,l}$ terms, can be computed using,

$$\beta_{i,l} = \left[\sum_{n=1}^{N} \left\{(s_{\text{npl}} - s_{\text{nml}})\omega_{rn}\right\}\right]^2 - \omega_{ri}^2, \qquad (7)$$

where the subscript l denotes the lth term of $\mathbf{u}^*$, written as u_l^* and s_{npl} and s_{nml} represent the power indices of u_{np} and u_{nm} of the term u_l^*, respectively. Finally the variable, r, that describes the ratio between the response frequencies of mode 2 and 3, i.e. $r = \omega_{r3}/\omega_{r2}$, is introduced, so that for the example considered here $\boldsymbol{\beta}$ is,

$$\mathbf{u}_v^* = \begin{bmatrix} u_{2p}^3 \\ u_{2p}^2 u_{2m} \\ u_{2p}u_{2m}^2 \\ u_{2m}^3 \\ u_{2p}u_{3p}^2 \\ u_{2p}u_{3p}u_{3m} \\ u_{2p}u_{3m}^2 \\ u_{2m}u_{3p}^2 \\ u_{2m}u_{3p}u_{3m} \\ u_{2m}u_{3m}^2 \\ u_{2p}^2 u_{3p} \\ u_{2p}u_{2m}u_{3p} \\ u_{2m}^2 u_{3p} \\ u_{2p}^2 u_{3m} \\ u_{2p}u_{2m}u_{3m} \\ u_{2m}^2 u_{3m} \\ u_{3p}^3 \\ u_{3p}^2 u_{3m} \\ u_{3p}u_{3m}^2 \\ u_{3m}^3 \\ u_{1p} \\ u_{1m} \\ u_{2p} \\ u_{2m} \\ u_{3p} \\ u_{3m} \end{bmatrix}, \mathbf{n}_v^T = \mu \begin{bmatrix} 0 & 1 & 0 \\ 0 & 3 & 0 \\ 0 & 3 & 0 \\ 0 & 1 & 0 \\ 0 & 27 & 0 \\ 0 & 54 & 0 \\ 0 & 27 & 0 \\ 0 & 27 & 0 \\ 0 & 54 & 0 \\ 0 & 27 & 0 \\ 0 & 0 & 9 \\ 0 & 0 & 18 \\ 0 & 0 & 9 \\ 0 & 0 & 9 \\ 0 & 0 & 18 \\ 0 & 0 & 9 \\ 0 & 0 & 27 \\ 0 & 0 & 81 \\ 0 & 0 & 81 \\ 0 & 0 & 27 \\ j\eta_1 & 0 & 0 \\ -j\eta_1 & 0 & 0 \\ 0 & j\eta_2 & 0 \\ 0 & -j\eta_2 & 0 \\ 0 & 0 & j\eta_3 \\ 0 & 0 & -j\eta_3 \end{bmatrix},$$

$$\boldsymbol{\beta}^T = \omega_{r2}^2 \begin{bmatrix} - & 8 & - \\ - & 0 & - \\ - & 0 & - \\ - & 8 & - \\ - & 4(r^2+r) & - \\ - & 0 & - \\ - & 4(r^2-r) & - \\ - & 4(r^2-r) & - \\ - & 0 & - \\ - & 4(r^2+r) & - \\ - & - & 4(1+r) \\ - & - & 0 \\ - & - & 4(1-r) \\ - & - & 4(1-r) \\ - & - & 0 \\ - & - & 4(1+r) \\ - & - & 8r^2 \\ - & - & 0 \\ - & - & 0 \\ - & - & 8r^2 \\ 0 & - & - \\ 0 & - & - \\ - & 0 & - \\ - & 0 & - \\ - & - & 0 \\ - & - & 0 \end{bmatrix},$$

where $\eta_i = 2\omega_{ni}\zeta_i/u$ and in β, a dash indicates that the value is insignificant since the corresponding coefficient in $\mathbf{n}_v$ is zero. The zero terms in β represent unconditionally resonant terms which have to be retained in $\mathbf{N}_u$. Furthermore, there are also additional conditionally resonant terms which are potentially set to zero depending on the value of r. For example, $r = 1$ will lead further zero terms in $\boldsymbol{\beta}$. For all the terms for which $\beta = 0$, the corresponding terms in $\mathbf{n}_v$ are set equal to those in $\mathbf{n}_u$.

The modal interaction case considered here is when $\omega_{n1} : \omega_{n2} : \omega_{n3} \approx 1 : 1 : 1$. This allows us to assume all modal fundamental response frequencies are at the forcing frequency, i.e. $\Omega = \omega_{r1} = \omega_{r2} = \omega_{r3}$, such that $r = 1$. Therefore, the terms in column 2, row 7 and 8 and column 3, row 13 and 14 in $\boldsymbol{\beta}$ become zero and the resulting dynamic equations of u_i are,

$$\ddot{u}_1 + 2\omega_{n1}\zeta_1\dot{u}_1 + \omega_{n1}^2 u_1 = P_{m1}\cos(\Omega t), \tag{8a}$$

$$\ddot{u}_2 + 2\omega_{n2}\zeta_2\dot{u}_2 + \omega_{n2}^2 u_2$$
$$+ 3\mu\Big[\big(u_{2p}^2 u_{2m} + u_{2p}u_{2m}^2\big)$$
$$+ 18\big(u_{2p}u_{3p}u_{3m} + u_{2m}u_{3p}u_{3m}\big)$$

$$+ 9\Big(u_{2m}u_{3p}^2 + u_{2p}u_{3m}^2\Big)\Big]$$
$$= P_{m2}\cos(\Omega t), \tag{8b}$$

$$\ddot{u}_3 + 2\omega_{n3}\zeta_3\dot{u}_3 + \omega_{n3}^2 u_3$$
$$+ 9\mu\Big[9(u_{3p}^2 u_{3m} + u_{3p}u_{3m}^2)$$
$$+ 2(u_{2p}u_{2m}u_{3p} + u_{2p}u_{2m}u_{3m})$$
$$+ (u_{2p}^2 u_{3m} + u_{2m}^2 u_{3p})\Big]$$
$$= P_{m3}\cos(\Omega t). \tag{8c}$$

Substituting $u_{ip} = (U_i/2)\,e^{j(\Omega t - \phi_i)}$ and $u_{im} = (U_i/2)\,e^{-j(\Omega t - \phi_i)}$, where U_i and ϕ_i are the fundamental response amplitude and phase of the ith mode, respectively, into Eq. 8 and balancing the coefficients of $e^{j\Omega t}$ and $e^{-j\Omega t}$, we obtain the time-invariant equations for the forced response of the system,

$$\Big\{(\omega_{n1}^2 - \Omega^2)^2 + (2\omega_{n1}\zeta_1\Omega)^2\Big\}U_1^2 = P_{m1}^2,$$

$$\left\{\left[\omega_{n2}^2 - \Omega^2 + \frac{3\mu}{4}(U_2^2 + (18 + 9p)U_3^2)\right]^2 \right.$$
$$\left. + (2\omega_{n2}\zeta_2\Omega)^2\right\}U_2^2 = P_{m2}^2$$

$$\left\{\left[\omega_{n3}^2 - \Omega^2 + \frac{9\mu}{4}(9U_3^2 + (2 + p)U_2^2)\right]^2 \right.$$
$$\left. + (2\omega_{n3}\zeta_3\Omega)^2\right\}U_3^2 = P_{m3}^2, \tag{9}$$

where $p = e^{j2(|\phi_2 - \phi_3|)}$. The $|\phi_2 - \phi_3|$ term represents the phase difference between mode 2 and 3.

To obtain the backbone curves, the unforced, undamped system needs to be considered. Therefore, by setting the damping and external force to be zero, i.e. $\zeta_i = 0$ and $P_{mi} = 0$, in Eq. 9 gives

$$\Big[-\Omega^2 + \omega_{n1}^2\Big]U_1 = 0, \tag{10a}$$

$$\left[-\Omega^2 + \omega_{n2}^2 + \frac{3}{4}\mu\left\{U_2^2 + (18 + 9p)U_3^2\right\}\right]U_2 = 0, \tag{10b}$$

$$\left[-\Omega^2 + \omega_{n3}^2 + \frac{9}{4}\mu\left\{9U_3^2 + (2 + p)U_2^2\right\}\right]U_3 = 0. \tag{10c}$$

Then successively setting (U_2 and U_3), (U_1 and U_3) and then (U_1 and U_2) to zero for Eq. 10 results in three single-mode backbone curve solutions labelled $S1$, $S2$

and $S3$

$$S1: \quad U_1 \neq 0, U_2 = U_3 = 0, \quad \Omega^2 = \omega_{n1}^2, \qquad (11)$$

$$S2: \quad U_2 \neq 0, U_1 = U_3 = 0,$$
$$\Omega^2 = \omega_{n2}^2 + \frac{3}{4}\mu U_2^2, \qquad (12)$$

$$S3: \quad U_3 \neq 0, U_1 = U_2 = 0,$$
$$\Omega^2 = \omega_{n3}^2 + \frac{81}{4}\mu U_3^2. \qquad (13)$$

Further observing Eq. 10, it can be seen that mode 1 is linear and not coupled with the other two modes, while modes 2 and 3 could potentially interact with each other. This modal interaction is also affected by the value of p. If u_2 and u_3 are both present, i.e. $U_2 \neq 0$ and $U_3 \neq 0$, Eq. 10b and 10c can be rearranged and set equal, so that

$$\Omega^2 = \omega_{n2}^2 + \frac{3}{4}\mu \left\{ U_2^2 + (18 + 9p)U_3^2 \right\}$$
$$= \omega_{n3}^2 + \frac{9}{4}\mu \left\{ 9U_3^2 + (2 + p)U_2^2 \right\}. \qquad (14)$$

To ensure Eq. 14 is real, the phase difference terms need to be, $p = \pm 1$. Here, $p = 1$ and $p = -1$ represent the in-unison and out-of-unison resonances, respectively. A detailed discussion describing how the value chosen of p and the corresponding resonant types can be found in [3,9]. Firstly, by setting $p = +1$ yields two extra backbone curves, labelled $S4^+$ and $S4^-$, with the phase difference

$$S4^+ : |\phi_2 - \phi_3| = 0, \qquad S4^- : |\phi_2 - \phi_3| = \pi, \quad (15)$$

and their corresponding backbone branch expressions are same and given as,

$$S4^\pm : \quad U_2^2 = \frac{\omega_{n2}^2 - \omega_{n3}^2}{6\mu}, \qquad (16a)$$

$$\Omega^2 = \frac{9\omega_{n2}^2 - \omega_{n3}^2}{8} + \frac{81}{4}\mu U_3^2. \qquad (16b)$$

The case where $p = -1$ yields two further backbone curves, denoted $S5^+$ and $S5^-$. They are characterised by the phase differences,

$$S5^+ : |\phi_2 - \phi_3| = +\pi/2, \qquad S5^- : |\phi_2 - \phi_3| = -\pi/2. \qquad (17)$$

Substituting $p = -1$ into Eq. 14 gives the response amplitude and frequency relationships,

$$S5^\pm : \quad U_2^2 = \frac{2(\omega_{n2}^2 - \omega_{n3}^2)}{3\mu} - 9U_3^2, \qquad (18a)$$

$$\Omega^2 = \frac{3\omega_{n2}^2 - \omega_{n3}^2}{2}. \qquad (18b)$$

From inspection of Eqs. 16a, 18a, it can be seen that, since $\omega_{n3} > \omega_{n2}$, the sign of μ must be negative for the equations to have real solutions such that the backbone branches are physically realisable.

3 Hardening case

3.1 Backbone curves

When the nonlinear stiffness is positive, $\mu > 0$, the solutions for Eqs. 16a and 18a are complex. Therefore, for the hardening case, the backbone branches $S4^\pm$ and $S5^\pm$ have no physical meaning and only $S1$, $S2$ and $S3$ exist. This means that there is no nonlinear modal interaction between the three backbone curves.

Figure 2 shows the backbones curves for the system with the hardening nonlinearity where $\omega_{n1} = 1$, $\omega_{n2} = 1.005$, $\omega_{n3} = 1.0015$ and the system parameters are $m = 1$, $k = 1$, $k' = 0.01$ and $\kappa = 0.05$. All panels show the backbone curves in the projection of the response frequency against the displacement. The panels in the first row show the amplitude of the fundamental components of the modal response, u_1, u_2 and u_3, and the second row shows the amplitude of the fundamental response of the physical displacement of mass 1 and 2, x_1 and x_2. Note that due to the system symmetry the backbone curve plot of mass 3 will be identical to that of mass 1 if it is shown. The $S1$, $S2$ and $S3$ branches are the single-mode backbone curves. It can be seen that $S1$ is linear and $S2$ and $S3$ show the characteristic shape of a hardening response.

3.2 Forced response

To show how the backbone curves can help facilitate the interpretation of the modal interaction of the nonlinear system, the forced response amplitude of three masses, X_1, X_2 and X_3, in the frequency domain for the hardening nonlinear system is shown in Fig. 3. To illustrate the relationship, the corresponding backbone curves in
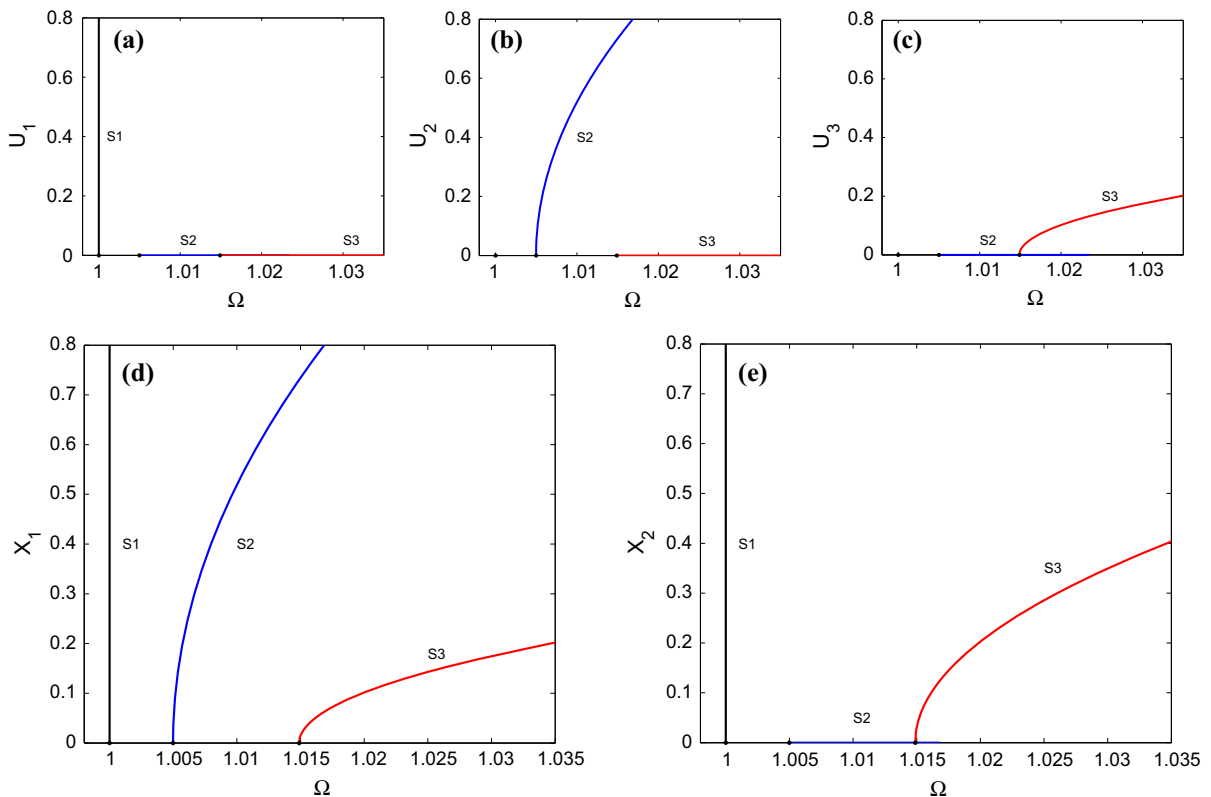
Fig. 2 Backbone curves for the nonlinear oscillator with the physical parameters $m = 1$, $k = 1$, $k' = 0.01$ and $\kappa = 0.05$, so the modal natural frequencies are $\omega_{n1} = 1$, $\omega_{n2} = 1.005$ and $\omega_{n3} = 1.015$. The panels in the *first row* show the modal dis-placement results, U_i, and those of the *second row* represent the backbone curve of the physical displacements of the mass 1 and 2, X_1 and X_2. The corresponding single-mode backbone curves are labelled by $S1$, $S2$ and $S3$

Fig. 2 are also shown. Here, a damping ratio $\zeta \simeq 0.001$ is chosen for all modes and the external force amplitude is $[P_1, P_2, P_3]^T = [3, -1, 1]^T \times 10^{-3}$, which corresponds to the situation where all three modes are excited at the same amplitude, i.e. $[P_{m1}, P_{m2}, P_{m3}]^T = [1, 1, 1]^T \times 10^{-3}$. The forced response has been computed from an initial steady state solution, found with numerical integration in MATLAB, which is then continued in forcing frequency using the software AUTO-07p [4].

From Fig. 3, it can be seen that the response curve can be divided into three parts from left to right by two minima,

- For the first resonance, the response curves of three masses are similar to that of the linear oscillator and are centred around $S1$.
- For the second resonance, the familiar shape of the responses of a typical Duffing oscillator are following $S2$ and the jump phenomenon can be also

observed on the right part of the curve for mass 1 and 3. Note that due to the special values of the linear modeshape of mode 2, i.e. $\{1, 0, -1\}^T$, there is no peak for the response of mass 2 in Fig. 3b within this bandwidth.

- For the third resonance, in Fig. 3a, the curve around $S3$ contains a loop where the upper trajectory is unstable which occurs from the addition and subtraction of the modal contributions. In Fig. 3b, c, the response of the typical Duffing oscillator can be observed enveloping $S3$.

For the first part of the response, mode 1 or linear mode, the resonant peak points are exactly on the linear backbone curve $S1$. For the other parts of the forced response curves, the curves cross the backbone curves $S2$ and $S3$ almost at the fold points. This is in line with the results found for systems with a lower number of degrees of freedom and shows how the backbone curves provide a good estimation of the position and

Fig. 3 Displacement amplitude of the three masses when the system is forced by the external force $[P_1, \ P_2, \ P_3] = [3, \ -1, \ 1] \times 10^{-3}$, corresponding to the modal force $[P_{m1}, \ P_{m2}, \ P_{m3}] = [1, \ 1, \ 1] \times 10^{-3}$, with system parameters $m = 1$, $k = 1$, $k' = 0.01$, $\kappa = 0.05$, $c = 0.002$ and $c' = 0$. The *blue solid lines* and *red dashed lines* represent the stable and unstable response, respectively. The *grey lines* represent backbone curves and the red stars represent fold points. (Color figure online)
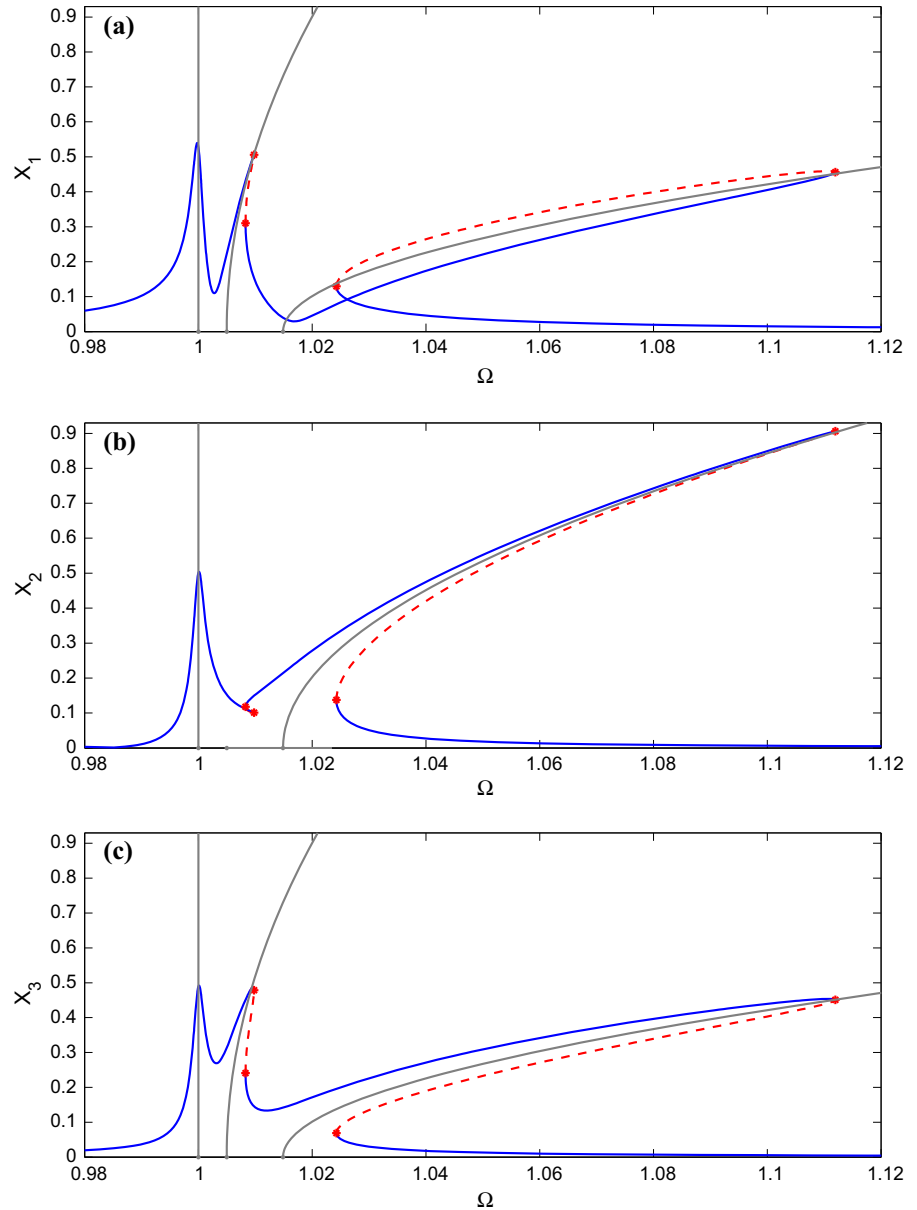
the shape of resonant peaks in the frequency amplitude plane.

4 Softening case

4.1 Backbone curves

For the softening case, $\mu < 0$, Eqs. 16a and 18a have real solutions. Therefore, the in-unison, $S4^{\pm}$, and out-of-unison, $S5^{\pm}$, resonant backbone curves are physi-

cal. In Fig. 4, the backbone curves for the softening case where $\omega_{n1} = 1$, $\omega_{n2} = 1.005$, $\omega_{n3} = 1.015$ and $\kappa = -0.05$ are shown. The first and second columns show the backbone curves of the modal states, u_1, u_2 and u_3, and the physical displacements, x_1, x_2 and x_3, respectively. As with the hardening case, the single-mode backbone curves, $S1$, $S2$ and $S3$, for mass 1 and 3 are the same. However, the symmetry is broken as the $S4^{\pm}$ comes with the position of $S4^+$ and $S4^-$ swapped. Here, the mixed-mode backbone curves $S4^{\pm}$ and $S5^{\pm}$,

where both mode 2 and 3 are activated, are of primary interest.

In Fig. 4, as expected the branch $S1$ is still a straight vertical line and $S2$ and $S3$ are curved, but with an opposite bending direction compared with those of the hardening system. Furthermore, it can be seen that $S4^{\pm}$ emanate from branch $S2$ and $S5\pm$ bifurcate from branch $S3$. This type of bifurcation phenomenon has been previously studied in other systems, see for example [3,9]. A significant difference from the previous systems in the literature is that the $S5^{\pm}$ here is a vertical straight backbone curve which means that, like a linear mode, the resonant frequencies will not vary with the response amplitude. Also the backbone curve $S5^{\pm}$ has a finite length and it ends at $S2$, which implies that the out-of-unison resonance only happens within a certain amplitude range for this example.

4.2 Stability of the backbone curve

We now consider the stability of the backbone curves. Here, only the stability analysis of the backbone branch $S2$ is given in detail due to the fact that both $S4^{\pm}$ and $S5^{\pm}$ intersect with it, as shown in Fig. 4. Note that on backbone curve $S2$ which is the solution of Eq. 12, u_3 is equal to zero. So the stability of $S2$ can be determined by considering the dynamics of u_3 about its zero solution (Note that u_1 is not considered here due to its independence of u_2 and u_3). When the zero solution of u_3 is unstable, the $S2$ solution is also unstable.

Now, the unforced, undamped equation of mode 3, Eq. 8c, is considered with setting $c_{m3} = 0$ and $P_{m3} = 0$, such that,

$$\ddot{u}_3 + \omega_{n3}^2 u_3 + 9\mu$$
$$\left[2u_{2p}u_{2m}u_3 + \left(u_{2p}^2 u_{3m} + u_{2m}^2 u_{3p} \right) \right] = 0. \quad (19)$$

As u_3 is considered around its zero solution, the $u_{3p}u_{3m}u_3$ term is so small that it has been neglected. The stability of the system is found by considering the amplitude and phase of u_3 to be a slowly varying functions of time using the parameter ε to denote 'smallness'. A similar treatment can also be seen in [28]. Combined with $u_i = u_{ip} + u_{im}$, we can write u_3 as

$$u_3 = u_{3p} + u_{3m} = \frac{U_{3p}(\varepsilon t)}{2} e^{j\omega_{r3}t} + \frac{U_{3m}(\varepsilon t)}{2} e^{-j\omega_{r3}t}. \quad (20)$$

Furthermore, the derivatives of u_3 can be written as,

$$\dot{u}_3 = j\omega_{r3} \left(\frac{U_{3p}(\varepsilon t)}{2} e^{j\omega_{r3}t} - \frac{U_{3m}(\varepsilon t)}{2} e^{-j\omega_{r3}t} \right)$$
$$+ \varepsilon \left(\frac{\dot{U}_{3p}(\varepsilon t)}{2} e^{j\omega_{r3}t} + \frac{\dot{U}_{3m}(\varepsilon t)}{2} e^{-j\omega_{r3}t} \right), \quad (21)$$

and

$$\ddot{u}_3 = -\omega_{r3}^2 u_3$$
$$+ 2j\omega_{r3}\varepsilon \left(\frac{\dot{U}_{3p}(\varepsilon t)}{2} e^{j\omega_{r3}t} - \frac{\dot{U}_{3m}(\varepsilon t)}{2} e^{-j\omega_{r3}t} \right)$$
$$+ \mathcal{O}(\varepsilon^2), \quad (22)$$

where order ε^2 terms have been neglected. Substituting the expression of $\ddot{u}_3$ into Eq. 19 and then balancing the coefficients of the $e^{j\omega_{r3}t}$ and $e^{-j\omega_{r3}t}$ terms gives,

$$\dot{U}_{3p} = -j \left(\frac{\omega_{r3}^2 - \omega_{n3}^2}{\omega_{r3}} \right) \frac{U_{3p}}{2}$$
$$+ j\frac{9\mu}{8\omega_{r3}} \left(2U_{2p}U_{2m}U_{3p} + U_{2p}^2 U_{3m} \right), \quad (23a)$$

and

$$\dot{U}_{3m} = j \left(\frac{\omega_{r3}^2 - \omega_{n3}^2}{\omega_{r3}} \right) \frac{U_{3m}}{2}$$
$$- j\frac{9\mu}{8\omega_{r3}} \left(2U_{2p}U_{2m}U_{3m} + U_{2m}^2 U_{3p} \right). \quad (23b)$$

Now these equations can be expressed in the form,

$$\dot{\mathbf{U}}_3 = \mathbf{f}_{\mathbf{U}_3}\mathbf{U}_3, \quad (24)$$

where $\mathbf{U}_3 = \{U_{3p}\ U_{3m}\}^T$ and the Jacobian matrix is,

$$\mathbf{f}_{\mathbf{U}_3} = \frac{j}{\omega_{r3}}$$
$$\begin{bmatrix} \frac{9\mu}{4}U_{2p}U_{2m} - \frac{\omega_{r3}^2 - \omega_{n3}^2}{2} & \frac{9\mu}{8}U_{2p}^2 \\ -\frac{9\mu}{8}U_{2m}^2 & -\frac{9\mu}{4}U_{2p}U_{2m} + \frac{\omega_{r3}^2 - \omega_{n3}^2}{2} \end{bmatrix}.$$

So the stability of the zero solution of u_3 can be assessed by considering the eigenvalues of the matrix, $\mathbf{f}_{\mathbf{U}_3}$, about the equilibrium solution $\mathbf{U}_3 = 0$. So, the eigenvalues,
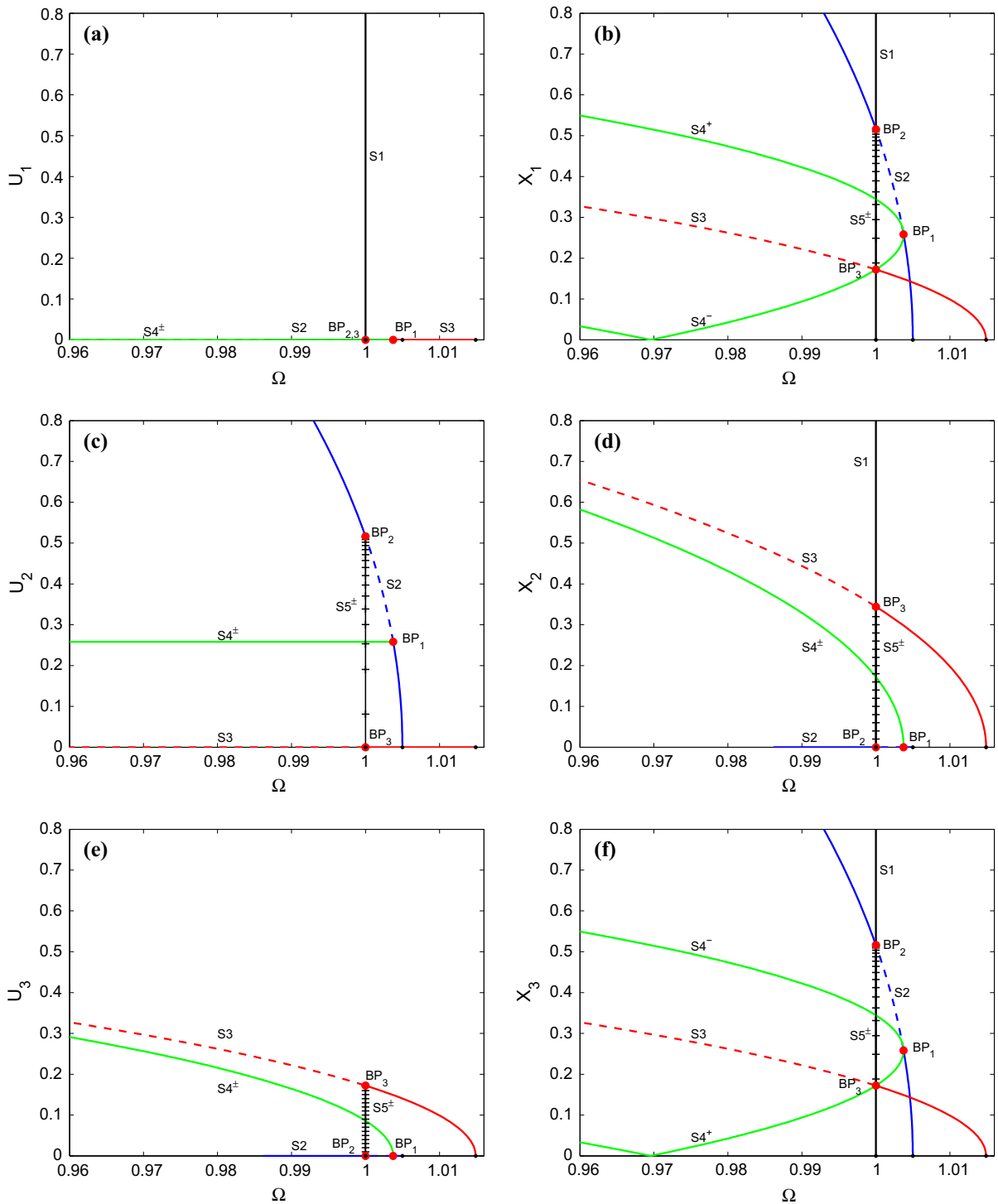
Fig. 4 Backbone curves for the oscillator with the physical parameters $k = 1$, $k' = 0.01$ and $\kappa = -0.05$, such that the modal natural frequencies are $\omega_{n1} = 1$, $\omega_{n2} = 1.005$ and $\omega_{n3} = 1.015$. The *panels* in the *first* and *second column* show the modal and physical displacement results, respectively. Stable solutions are shown with the *solid lines*, whereas unstable solutions are represented by the *dashed lines*. Bifurcation points are noted by BP_i. Note that due to the identical natural frequencies, the branches $S5^{\pm}$ overlap with $S1$, so the $S5^{\pm}$ backbone curves are indicated by the *short cross lines* for distinction

λ, are given by,

$$\omega_{r3}^2\lambda^2 + \left(\frac{9\mu}{4}U_2^2 - \frac{\omega_{r3}^2 - \omega_{n3}^2}{2}\right)^2 - \left(\frac{9\mu}{8}U_2^2\right)^2 = 0, \tag{25}$$

where $U_2^2 = U_{2p}U_{2m}$ has been used. From inspecting the above equation, it can be seen that the values of λ can be only be either purely imaginary or real. When all the eigenvalues, λ, are purely imaginary the system is marginally stable, while when λ are real the system is unstable. This implies that the bifurcation point on the backbone curve occurs when both of the roots of Eq. 25 are zero, such that,

$$\left|\frac{9\mu}{4}U_2^2 - \frac{\omega_{r3}^2 - \omega_{n3}^2}{2}\right| = \left|\frac{9\mu}{8}U_2^2\right|. \tag{26}$$

Then using the expression for $S2$ given in Eq. 12 gives the bifurcation points,

$$BP_1: \ \Omega^2 = \frac{9\omega_{n2}^2 - \omega_{n3}^2}{8} \ \& \ U_2^2 = \frac{\omega_{n2}^2 - \omega_{n3}^2}{6\mu}, \quad (27)$$

and

$$BP_2: \ \Omega^2 = \frac{3\omega_{n2}^2 - \omega_{n3}^2}{2} \ \& \ U_2^2 = \frac{2(\omega_{n2}^2 - \omega_{n3}^2)}{3\mu}. \tag{28}$$

These are the same points where $S4^{\pm}$ and $S5^{\pm}$ intersect with $S2$, respectively. Note that since the linear natural frequencies of the modes are similar, the resonant response of the second and third modes will be at the same frequency. Hence, here, the relationship $\omega_{r3} = \omega_{r2} = \Omega$ has been used to simplify the equations.

Using the same approach, it can be also shown that the parts of $S2$ below bifurcation point BP_1 and above BP_2 are stable and the part between the two bifurcation points is unstable.

The same method was also used to predict that on $S3$ there is another bifurcation point,

$$BP_3: \ \Omega^2 = \frac{3\omega_{n2}^2 - \omega_{n3}^2}{2} \ \& \ U_3^2 = \frac{2(\omega_{n2}^2 - \omega_{n3}^2)}{27\mu}, \tag{29}$$

which is the intersection point of $S3$ and $S5^{\pm}$. Also the stability condition of branch $S3$ is that the part below BP_3 is stable and the section above is unstable. All these bifurcation points are also shown in Fig. 4. Using bifurcation theory for Hamiltonian systems and comparing with other similar systems in the published literature, all the bifurcation points here are (Hamiltonian) pitchfork bifurcations [3,7,25].

4.3 Analysis of the forced response

4.3.1 Forced response

We now examine the relationship between the forced response and the backbone curves for the softening nonlinear case. From the backbone curve results, it can be seen that the modal interactions occur for this case. Therefore, a simple forced configuration where only mode 2 is excited is chosen as two kinds of interactions bifurcate from backbone curve $S2$. For this forcing configuration, three different force amplitudes are chosen which are $[P_{m1}, \ P_{m2}, \ P_{m3}] = [0, 0.4, 0] \times 10^{-3}$, $[0, 0.9, 0] \times 10^{-3}$ and $[0, 1.5, 0] \times 10^{-3}$ and the damping ratio is chosen to be $\zeta = 0.001$.

Figure 5 shows the forced response results superimposed on the backbone curves for mass 1.

– For the small force amplitude situation, Fig. 5a, there is only one response curve which is centred around $S2$. This curve is the response of a typical softening Duffing oscillator and only composed the response of mode 2, u_2. For this case, the force is insufficient to trigger the modal interaction or jump.

– For the medium force amplitude situation, Fig. 5b, there are three response curves (1 blue and 2 green). The two green curves following $S4^{\pm}$ bifurcate from the single-mode response curve (blue one) at two secondary bifurcation points, respectively, and they are composed of the response of both mode 2, u_2, and mode 3, u_3.

– For the large force amplitude situation, Fig. 5c, there are two additional response curves (the black ones) surrounding $S5^{\pm}$ which also bifurcates from the single-mode response curve of mode 2. On these two curves, both mode 2 and 3 are present as well.

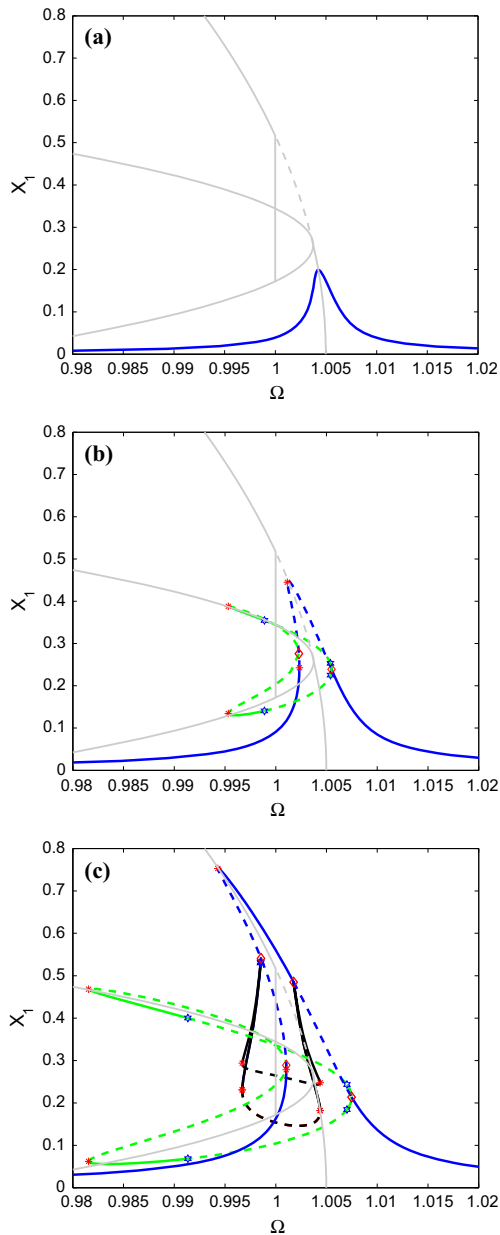From the results in Fig. 5, it can be noticed that for the situation where only one nonlinear mode is directly

Fig. 5 Displacement amplitude of the first mass when the system is excited in only the second mode at three different force amplitudes **a** $[P_{m1}, P_{m2}, P_{m3}] = [0, 0.4, 0] \times 10^{-3}$, **b** $[P_{m1}, P_{m2}, P_{m3}] = [0, 0.9, 0] \times 10^{-3}$ and **c** $[P_{m1}, P_{m2}, P_{m3}] = [0, 1.5, 0] \times 10^{-3}$) with system parameters $m = 1$, $k = 1$, $k' = 0.01$, $\kappa = -0.05$, $c = 0.002$ and $c' = 0$. The *diamonds*, *stars* and *asterisks* indicate secondary bifurcation, torus bifurcation and fold points. The *blue*, *green* and *black solid lines* and *dashed lines* represent the stable and unstable displacement response, respectively. The *grey lines* represent the backbone curves. Note that as forcing is in the second mode only, the backbone branches *S1* and *S3* have not been plotted here. (Color figure online)

excited the magnitude of the force amplitude may affect the occurrence of the modal interaction. More specifically, some critical values of the force amplitude must be reached to result in the modal interaction. Furthermore, the mixed-mode responses following the in-unison backbone curves would be triggered prior to those for the out-of-unison backbone curves when the external force amplitude increases.

4.3.2 Discussion of the force amplitude for triggering the modal interaction

Now, we consider at what forcing amplitude the modal interaction is triggered for the single-mode excitation situation. In Fig. 5b, c, it can be seen that the mixed-mode response curves emanate from the single-mode response curve at the secondary bifurcation points. We infer from this that the modal interaction response curves will appear from the single-mode response curve when only one linear mode is forced [2,9]. So, the existence of modal interaction is studied by looking for bifurcation points on the single-mode response curve. The theory used for detecting the secondary bifurcation points is the same used for the stability of backbone curves in Sect. 4.2. When the zero solution for the response of the unforced mode is stable (unstable), the single-mode response curve of the other forced mode is also stable (unstable). As a result the point of neutral stability is the secondary bifurcation point. The case where only mode 2 is forced has been considered as an example here. Along the response curve composed of only u_2 (blue curves in Fig. 5), the modal coordinate u_3 is zero, so we are going to study the stability of the zero solution of u_3 [6].

Firstly, substituting trial solutions for u_3, $\dot{u}_3$ and $\ddot{u}_3$, Eqs. 20, 21 and 22, into Eq. 8c with $P_{m3} = 0$ (as only mode 2 is forced) and $\omega_{r3} = \Omega$ (as the fundamental components of all modal responses of this system are at the force frequency). Note that here an accuracy of order ε^1 is considered. As the damping is assumed to be small which allows us to regard ζ_i to be order ε^1, so the second expression part of Eq. 21 can be ignored after implying the damping coefficient. Then balancing $e^{j\Omega t}$ and $e^{-j\Omega t}$, the equations of $\mathbf{U_3} = \{U_{3p} \ U_{3m}\}^T$ can be obtained as,

$$\dot{\mathbf{U}}_3 = F_{U_3} U_3 \tag{30}$$

where

$$\mathbf{F_{U_3}} = \begin{bmatrix} \dfrac{\Omega^2 - \omega_{n3}^2 - \frac{9\mu}{2}U_{2p}U_{2m} - j2\omega_{n3}\zeta_3\Omega}{2j\Omega} & -\dfrac{9\mu U_{2p}^2}{8j\Omega} \\[3mm] \dfrac{9\mu U_{2m}^2}{8j\Omega} & \dfrac{\Omega^2 - \omega_{n3}^2 - \frac{9\mu}{2}U_{2p}U_{2m} + j2\omega_{n3}\zeta_3\Omega}{-2j\Omega} \end{bmatrix}.$$

Then the eigenvalues, λ, for $\mathbf{F_{U_3}}$ can be obtained from,

$$\hat{a}\lambda^2 + \hat{b}\lambda + \hat{c} = 0, \tag{31}$$

where

$$\hat{a} = 4\Omega^2,$$
$$\hat{b} = 8\omega_{n3}\zeta_3\Omega^2,$$

and

$$\hat{c} = (\Omega^2 - \omega_{n3}^2)^2 - 9\mu U_2^2(\Omega^2 - \omega_{n3}^2)$$
$$+ \frac{243}{16}U_2^4 + (2\omega_{n3}\zeta_3\Omega)^2.$$

Therefore, the stability of the zero solution, $U_3 = 0$, can be determined from the eigenvalues, λ_i, $i = 1, 2$. The roots of Eq. 31 are given by,

$$\lambda_{1,2} = \frac{-\hat{b} \pm \sqrt{(\hat{b}^2 - 4\hat{a}\hat{c})}}{2\hat{a}}. \tag{32}$$

For all parameter values in this example $\hat{a}$ and $\hat{b}$ are positive. So when one of the eigenvalues is zero and another is negative real, the system is neutrally stable. Therefore, the bifurcation occurs when $\hat{c}$ is zero, such that,

$$243\mu^2 U_2^4 - 144\mu(\Omega^2 - \omega_{n3}^2)U_2^2$$
$$+ 16\left[(\Omega^2 - \omega_{n3}^2)^2 + (2\omega_{n3}\zeta_3\Omega)^2\right] = 0. \tag{33}$$

Combining Eq. 33 with the equation for the single-mode response curve for u_2 obtained by setting $U_3 = 0$ in Eq. 8(b) expressed as below,

$$9\mu^2 U_2^6 + 24\mu(\omega_{n2}^2 - \Omega^2)U_2^4$$
$$+ 16\left[(\omega_{n2}^2 - \Omega^2)^2 + (2\omega_{n2}\zeta_2\Omega)^2\right]U_2^2 = 16P_{m2}^2, \tag{34}$$

it allows us to find the position and number of their intersection points. To ensure the solutions are physically reasonable, only the intersection points at $U > 0$

and $\Omega > 0$ are considered. Those points are secondary bifurcation points that can be used to predict the onset of the modal interaction.

There are three possible cases:

(1) if there is zero or one intersection point, there will be no modal interaction. Fig. 6a.
(2) if there are two or three intersection points, the modal interaction response following the in-unison backbone curves will exist. Fig. 6b.
(3) if there are four intersection points, both the modal interaction response following the in-unison and out-of-unison backbone curves will occur. Figure 6c.

Figure 6 shows the curves of Eqs. 33 (red) and 34 (green) with the same parameter values of the system shown in Fig. 5, and their intersection points are marked by red dots. To make a comparison, the corresponding response curves (black) in Fig. 5 are also shown here. From Fig. 6, it can be seen that the single-mode response curve results approximated using the normal form technique and those calculated by AUTO are in good agreement. In addition, the intersections of Eqs. 33 and 34 are very close to the secondary bifurcation points for every case. The results show that the analytical method presented in this paper can be applied to detect the occurrence of modal interaction and identify the position of bifurcation points.

Furthermore, when only mode 3 is excited, the same analysis method can be applied to find the bifurcation points at the single-mode response curve composed of only u_3. This leads to two equations below,

$$2187\mu^2 U_3^4 - 432\mu(\Omega^2 - \omega_{n2}^2)U_3^2$$
$$+ 16\left[(\Omega^2 - \omega_{n2}^2)^2 + (2\omega_{n2}\zeta_2\Omega)^2\right] = 0, \tag{35}$$

and

$$6561\mu^2 U_3^6 + 648\mu(\omega_{n3}^2 - \Omega^2)U_3^4$$
$$+ 16\left[(\omega_{n3}^2 - \Omega^2)^2 + (2\omega_{n3}\zeta_3\Omega)^2\right]U_3^2 = 16P_{m3}^2. \tag{36}$$

Similarly, combining Eqs. 35 and 36 to find the position and number of their intersection points, we can predict the occurrence of modal interaction for the only mode 3 forced situation. Figure 7 shows the position relationship between these two curves of the
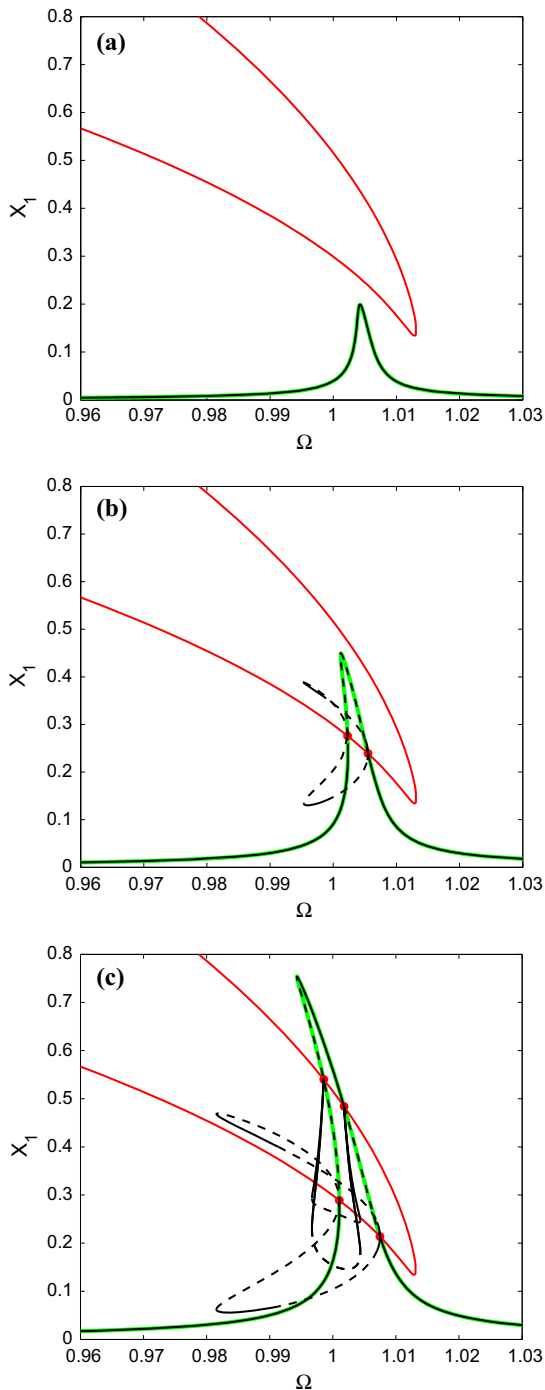
Fig. 6 The curves of Eqs. 33 (red) and 34 (green) for three different magnitudes of force amplitude cases: **a** $P_{m2} = 0.4 \times 10^{-3}$, **b** $P_{m2} = 0.9 \times 10^{-3}$ and **c** $P_{m2} = 1.5 \times 10^{-3}$. The system parameters are: $\omega_{n2} = 1.005$, $\omega_{n3} = 1.015$, $\mu = -0.05$, and $\zeta \approx 0.001$. The *red dots* mark the intersection points and the *black solid* and *dashed curves* represent the stable and unstable force response curves generated using AUTO. (Color figure online)

softening system for two force amplitude situations: $P_{m3} = 0.5 \times 10^{-3}$ and $P_{m3} = 1.0 \times 10^{-3}$. The intersection points are marked by red dots. The corresponding backbone curves $S3$ and $S5^{\pm}$ in Fig. 4 and response curves computed by AUTO are also shown to make the comparison.

For the two forced situations, there are zero intersection point, in Fig. 7a, and two intersection points, in Fig. 7b, between curves of Eqs. 35 and 36, respectively. As expected, there is no mixed-mode response in Fig. 7a. In Fig. 7b, it can be seen that the mixed-mode response curves following $S5^{\pm}$ emanate from the single-mode response curve from the intersection points. In fact, as there is only one intersection point between the backbone curve $S3$ and the curve of Eq. 36, the single-mode response curve of u_3, Eq. 35, can intersect with the curve of Eq. 36 at two points at most in the interesting frequency range. This means that only one kind of mixed-mode resonant responses which is the one following $S5^{\pm}$ shown in the results may bifurcate from the single-mode response curve of u_3 when the linear mode 3 of the system is excited. This is also in agreement with the expectation of the backbone curve results that only the out-of-unison resonant backbone curves $S5^{\pm}$ emanate from $S3$.

5 Conclusion

In this paper, we have considered the $N-1$ modal interactions that occur in a three-degree-freedom lumped mass system. In particular we considered the potential modal interactions of the system by analysing the backbone curves of the undamped, unforced system. This is an important topic because in lightly damped structures the dynamic behaviour is largely determined by the properties of the underlying undamped dynamic system.

First the undamped, unforced case was considered. In particular the modal interaction case that occurs when all the underlying linear modal frequencies are close was examined (i.e. $\omega_{n1} : \omega_{n2} : \omega_{n3} \approx 1 : 1 : 1$). In this case the first mode is linear because of the symmetry of the system and the other two modes will potentially interact with each other when the special parameters are chosen. We showed how this system can be analysed using a normal form transformation to obtain the nonlinear backbone curves of the undamped, unforced response. Following this, the response in the
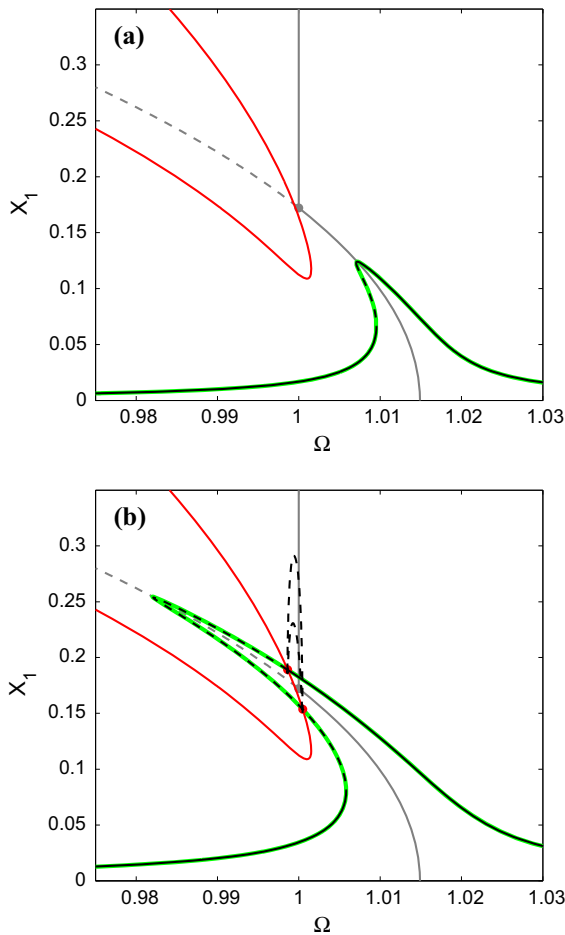
Fig. 7 The curves of Eq. 35 (*red*) and Eq. 36 (*green*) for two different magnitudes of force amplitude cases: **a** $P_{m3} = 0.5 \times 10^{-3}$ and **b** $P_{m3} = 1.0 \times 10^{-3}$. The system parameters are: $\omega_{n2} = 1.005$, $\omega_{n3} = 1.015$, $\mu = -0.05$, and $\zeta \approx 0.002$. The *red dots* mark the intersection points. The *grey curves* represent the corresponding backbone curves $S3$ and $S5^{\pm}$ and *black solid* and *dashed curves* represent the stable and unstable forced response curves generated using AUTO. (Color figure online)

frequency domain of the corresponding lightly damped and harmonically forced system was obtained using the continuation software AUTO-07p. This results were compared with the backbone curves to show its validity for predicting the nonlinear resonant behaviour of the system during $N - 1$ modal interactions.

References

1. Amabili, M.: Nonlinear Vibrations and Stability of Shells and Plates, vol. 257. Cambridge University Press, Cambridge (2008)
2. Arnol'd, V.I.: Geometrical methods in the theory of ordinary differential equations. Springer, New York (1988)
3. Cammarano, A., Hill, T.L., Neild, S.A., Wagg, D.J.: Bifurcations of backbone curves for systems of coupled nonlinear two mass oscillator. Nonlinear Dyn. **77**(1–2), 311–320 (2014)
4. Doedel E.J., Champneys A.R., Fairgrieve T.F., Kuznetsov Y.A, Dercole F., Oldeman B.E., Paffenroth R.C., Sandstede B., Wang X.J., Zhang C.: AUTO-07P: continuation and bifurcation software for ordinary differential equations. Montreal, Canada: Concordia University. http://cmvl.cs.concordia.ca (2008)
5. Gatti, G., Brennan, M.J., Kovacic, I.: On the interaction of the responses at the resonance frequencies of a nonlinear two degrees-of-freedom system. Phys. D: Nonlinear Phenomena **239**(10), 591–599 (2010)
6. Gonzalez-Buelga, A., Neild, S., Wagg, D., Macdonald, J.: Modal stability of inclined cables subjected to vertical support excitation. J. Sound Vib. **318**(3), 565–579 (2008)
7. Guckenheimer, J., Holmes, P.: Nonlinear Oscillations, Dynamical Systems, and Bifurcations of Vector Fields, vol. 42. Springer, Berlin (1983)
8. Haddow, A., Barr, A., Mook, D.: Theoretical and experimental study of modal interaction in a two-degree-of-freedom structure. J. Sound Vib. **97**(3), 451–473 (1984)
9. Hill, T., Cammarano, A., Neild, S., Wagg, D.: Out-of-unison resonance in weakly nonlinear coupled oscillators. In: Proceedings of the Royal Society of London A: Mathematical, Physical and Engineering Sciences, vol. 471, paper. 20140659. The Royal Society (2015)
10. Hill, T., Cammarano, A., Neild, S., Wagg, D.: Interpreting the forced responses of a two-degree-of-freedom nonlinear oscillator using backbone curves. J. Sound Vib. **349**, 276–288 (2015)
11. Jézéquel, L., Lamarque, C.H.: Analysis of non-linear dynamical systems by the normal form theory. J. Sound Vib. **149**(3), 429–459 (1991)
12. Kerschen, G., Kowtko, J.J., McFarland, D.M., Bergman, L.A., Vakakis, A.F.: Theoretical and experimental study of multimodal targeted energy transfer in a system of coupled oscillators. Nonlinear Dyn. **47**(1–3), 285–309 (2007)
13. Kerschen, G., Peeters, M., Golinval, J.C., Vakakis, A.F.: Nonlinear normal modes, part i: a useful framework for the structural dynamicist. Mech. Syst. Signal Process. **23**(1), 170–194 (2009)

14. Lamarque, C.H., Touzé, C., Thomas, O.: An upper bound for validity limits of asymptotic analytical approaches based on normal form theory. Nonlinear Dyn. **70**(3), 1931–1949 (2012)
15. Lewandowski, R.: On beams membranes and plates vibration backbone curves in cases of internal resonance. Meccanica **31**(3), 323–346 (1996)
16. Nayfeh, A.H.: Nonlinear Interactions. Wiley, Hoboken (2000)
17. Nayfeh, A.H., Balachandran, B.: Modal interactions in dynamical and structural systems. Appl. Mech. Rev. **42**(11S), S175–S201 (1989)
18. Nayfeh, A.H., Mook, D.T.: Nonlinear Oscillations. Wiley, Hoboken (2008)
19. Nayfeh, A.H., Pai, P.F.: Linear and Nonlinear Structural Mechanics. Wiley, Hoboken (2008)
20. Neild, S., Wagg, D.: A generalized frequency detuning method for multidegree-of-freedom oscillators with nonlinear stiffness. Nonlinear Dyn. **73**(1–2), 649–663 (2013)
21. Neild, S.A., Wagg, D.J.: Applying the method of normal forms to second-order nonlinear vibration problems. Proc. R. Soc A: Math., Phys. Eng. Sci. **467**(2128), 1141–1163 (2011)
22. Pierre, C., Jiang, D., Shaw, S.: Nonlinear normal modes and their application in structural dynamics. Math. Probl. Eng. **2006**, 1–15 (2006)
23. Rand, R.H.: Nonlinear normal modes in two-degree-of-freedom systems. J. Appl. Mech. **38**(2), 561–561 (1971)
24. Rega, G., Lacarbonara, W., Nayfeh, A., Chin, C.: Multiple resonances in suspended cables: direct versus reduced-order models. Int. J. Non-Linear Mech. **34**(5), 901–924 (1999)
25. Thompson, J.M.T., Stewart, H.B.: Nonlinear Dynamics and Chaos. Wiley, Hoboken (2002)
26. Touzé, C., Amabili, M.: Nonlinear normal modes for damped geometrically nonlinear systems: application to reduced-order modelling of harmonically forced structures. J. Sound Vib. **298**(4), 958–981 (2006)
27. Touzé, C., Thomas, O., Chaigne, A.: Asymmetric non-linear forced vibrations of free-edge circular plates. part 1: theory. J. Sound Vib. **258**(4), 649–676 (2002)
28. Wagg, D., Neild, S.: Nonlinear Vibration with Control: for Flexible and Adaptive Structures, vol. 218. Springer, Berlin (2014)
29. Xin, Z., Neild, S., Wagg, D., Zuo, Z.: Resonant response functions for nonlinear oscillators with polynomial type nonlinearities. J. Sound Vib. **332**(7), 1777–1788 (2013)